Bending Loss in Multimode Fibers with Graded and Ungraded Core Index

D. Gloge

Parabolic grading of the core index in a multimode fiber (Selfoc) diminishes mode dispersion and interface loss. This paper shows that this grading affects the mode volume and the loss in bends very little, if the index difference of the graded core (between the core axis and the cladding) is twice that of the homogeneous core. Curvature radii of several centimeters are tolerable. Mode coupling (or ray deflection) in random bends is slightly decreased by grading. Both the graded and the homogeneous multimode fiber are particularly sensitive to certain critical deviations of the guide axis from straightness. These deviations must be less than a fraction of a micrometer in order that catastrophic mode loss be avoided.

I. Introduction

Spatially incoherent light—from luminescent diodes, for example—requires multimode fibers for efficient transmission. Typically, these fibers consist of a glass core surrounded by a cladding of slightly lower refractive index. In the simplest case, the core material is homogeneous and has a flat index profile with an index step $n\Delta$ at the core–cladding interface, as shown in Fig. 1(a).

A multimode fiber of this kind has two disadvantages: (1) scatter loss produced by imperfections in the core–cladding interface and (2) delay distortion of the signal arising from pathlength differences among the possible propagation directions [see rays in Fig. 1(a)]. Light, for example, which requires a propagation time T on axis, is delayed by $(1 + \Delta)T$ if it propagates at the critical angle.

An inhomogeneous core with a parabolic index profile [Fig. 1(b)] alleviates these problems. Its practical realization looks more difficult at first glance,[1,2] but with ion exchange, deposition and doping techniques becoming common practice in fiber manufacture, there is reason to believe that, some day, the graded (parabolic) profile can be achieved as easily as the flat one. The graded profile provides continuous focusing to the light, so that the energy is concentrated along the axis, and little of it reaches the interface. Pathlength differences among the various propagation paths are compensated by velocity variations across the core region leaving very little delay distortion. In fact, the parabolically graded fiber, whose index decreases by $n\Delta$ across the core, exhibits only a delay difference of the order $T\Delta^2$ during the total propagation time T.[3,4] This means an improvement of almost two orders of magnitude over the flat profile for typical index differences Δ of the order of 1%.

The major disadvantage of the parabolic index profile has hitherto been seen in its performance in bends. This notion stems partly from bending loss computations and partly from ray tracing studies.[5–13] We show here that, for multimode transmission, this inferiority of the graded core is not very significant. A graded core, which has the same radius and twice the index difference of the homogeneous core, shows an at least equivalent performance in bends. As far as mode coupling in bends is concerned, the graded core seems even superior to the homogeneous one. We arrive at this conclusion by computing the bending losses for arbitrary mode numbers, linking these results to an equivalent ray representation and then performing a ray study in a randomly curved guide. Following previous studies[5–13] we derive most relations for the two-dimensional model—a curved thin film, for example. By using some obvious correspondence, we then apply these relations to the cylindrical guide.

II. Mode Volume and Mode-Ray Equivalence

The directions of propagation in the homogeneous core [see Fig. 1(a)] are limited by the critical angle for total internal reflection, which, because of Snell's law is

$$\theta_c = [1 - (n_c/n)^2]^{\frac{1}{2}} \approx (2\Delta)^{\frac{1}{2}}. \quad (1)$$

Here, as in the following, we assume that the difference between the cladding index n_c and the core index n is small, so that the approximation (1) holds. In that

The author is with Bell Telephone Laboratories, Inc., Crawford Hill Laboratory, Holmdel, New Jersey 07733.

Received 1 May 1972.

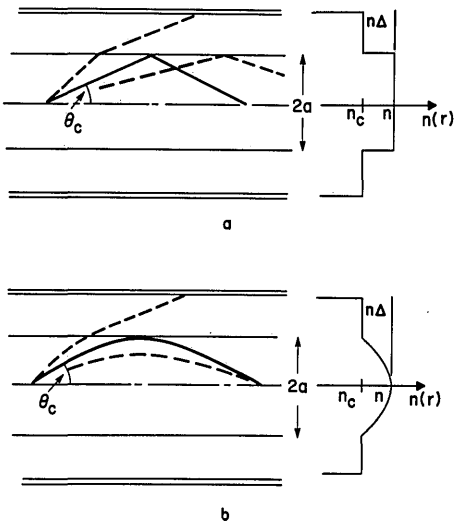

Fig. 1. Sketch of two cladded multimode fibers (a) with a homogeneous core and (b) with a graded core (parabolic index profile). The broken lines show possible guided and unguided rays. The critical ray is indicated by a solid line.

case, the total number of modes propagating in the cylindrical homogeneous core of radius a is

$$P_f = \tfrac{1}{2}(akn\theta_c)^2 = (akn)^2\Delta, \tag{2}$$

where $k = 2\pi/\lambda$ is the free-space propagation constant.[14]

An equivalent definition for the graded core can be obtained by considering the on-axis angle of a ray that just grazes the core–cladding interface [see Fig. 1(b)]. For a highly overmoded guide, this again is the angle limiting the possible directions of propagation. If the index profile is given by

$$n(r) = n[1 - \Delta(r^2/a^2)], \tag{3}$$

all rays follow sinusoidal paths of period $2\pi a/(2\Delta)^{\frac{1}{2}}$, a ray of amplitude a therefore forms an angle $(2\Delta)^{\frac{1}{2}}$ with the axis. The number of modes this guide transmits has been computed in Ref. 15, using a phase-space consideration. Since each volume element λ^2 in phase space is occupied by two modes of orthogonal polarization, the number of modes in a cylindrical core of radius a becomes

$$P_g = (akn)^2(\Delta/2) = \mathrm{P}_f 12 \tag{4}$$

for the parabolic profile.[15] The mode volume of both fibers becomes the same, if the index difference Δ of the graded profile is twice that of the flat profile.

For later use we need a correspondence relation between modes and their representative rays. We shall consider the two-dimensional case and describe rays by the angle θ at which they intersect the guide axis (Fig. 1). To obtain a relation between the mode number p and the angle θ, we use the same approach as in the three-dimensional case, and obtain

$$p_f = (2akn/\pi)\,\theta \tag{5}$$

for the flat profile and

$$p_g = (akn/2)\,\theta \tag{6}$$

for the graded profile. In the case of the homogeneous core, θ can be understood as the angle of propagation for the plane waves that constitute this mode in the core. In agreement with most of the literature, the expressions (5) and (6) for the two-dimensional case count only one of the two possible directions of polarization.

III. Curvature Loss

The following study of the radiation loss in bends is based on the results by Miller and Marcatili[6] and a refinement by Shevchenko.[7] A straightforward extension of their arguments leads to the following loss formula for a mode of propagation constant β, which is not too far from cutoff:

$$\alpha = 2\,\frac{\gamma^2(0)}{\beta}\exp\left[-2\int_a^{r_0}\gamma(r)d\right], \tag{7}$$

where

$$\gamma^2(r) = \beta^2R^2/(r + R)^2 - n_c^2k^2, \tag{8}$$

$$r_0 = R\beta/n_ck - R, \tag{9}$$

and R is the curvature radius. To interpret this result, we must first note that, for the straight guide, the mode field decreases as $\exp[-\gamma(0)(r - a)]$ in the cladding. For this reason, a loss mechanism in the cladding at a distance r from the guide axis—a scatter center or a lossy jacket—produces a loss for this mode that is proportional to $\exp[-2\gamma(0)(r - a)]$.

The curvature of the guide has two effects: First, the stretching of the waveguide at the outside of the bend leads to a velocity increase in the outer wing of the mode and hence to an apparent decrease of the propagation constant there (see Fig. 2). As a result, β has to be replaced by $\beta R/(r + R)$; the mode field now decreases as[7]

$$\exp\left[-\int_a^r \gamma(r)dr\right].$$

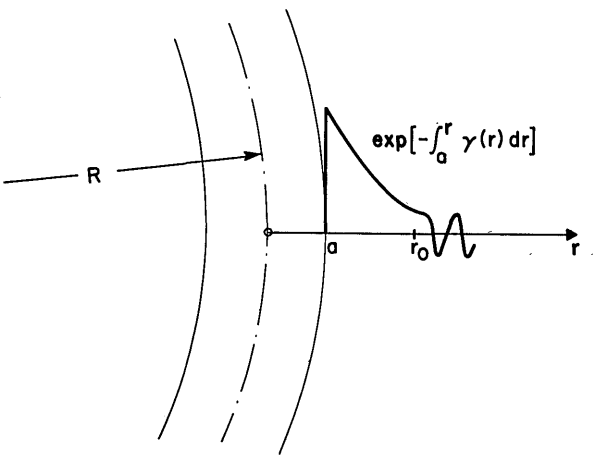

Fig. 2. Curved dielectric guide and its cladding field distribution at the outside of the bend (after Shevchenko[7]).

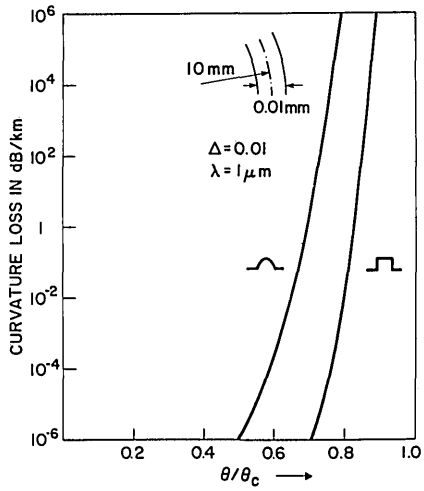

Fig. 3. Curvature loss in dB/km vs the relative mode angle for the graded and the flat index profile. Core diameter 0.1 mm, curvature radius $R = 1$ cm, wavelength $\lambda = 1\ \mu$m, relative index difference $\Delta = 1\%$.

Second, a loss mechanism arises at $r = r_0$, where the mode velocity reaches the velocity of light in the cladding material [$\gamma(r_0) = 0$]. The mode energy passing this radius is radiated off. The resulting loss leads to the exponential term in Eq. (7).

To solve Eq. (7) we rewrite Eq. (8) in the approximate form

$$\gamma^2(r) = \gamma^2(0) - 2\beta^2 r/R. \tag{10}$$

Here the fact has been used that $r < R\Delta \ll R$ in the entire range of integration. As an additional approximation, we replace β by nk. We then insert Eq. (10) into Eq. (7) and solve the integral. The result is

$$\alpha = 2\frac{\gamma^2(0)}{nk}\exp\left[-\frac{2}{3}nkR\left(\frac{\gamma^2(0)}{n^2k^2} - \frac{2a}{R}\right)^{3/2}\right]. \tag{11}$$

The exponential function in this expression agrees with the corresponding result of Ref. 5, which was obtained by an entirely different method.

To evaluate Eq. (11) in the case of the flat profile, we use the well-known relation for the propagation constant

$$\beta_f^2 = (nk)^2 - (\pi p_f/2a)^2 \tag{12}$$

with p_f from Eq. (5). Using also Eqs. (1) and (8), we obtain

$$\gamma_f^2(0) = (nk)^2(\theta_c^2 - \theta^2). \tag{13}$$

The loss of a mode, which corresponds to a ray at angle θ, is therefore

$$\alpha_f = 2nk(\theta_c^2 - \theta^2)\exp\left[-\tfrac{2}{3}nkR\left(\theta_c^2 - \theta^2 - \frac{2a}{R}\right)^{3/2}\right]. \tag{14}$$

As mentioned earlier, this derivation applies only to high order modes (not too far from cutoff); the case $\theta \ll \theta_c$ is not covered.

For the graded profile, we have

$$\beta_g = nk - \frac{(2\Delta)^{\frac{1}{2}}(p_g + \frac{1}{2})}{a} \tag{15}$$

with p_g from Eq. (6). Using again Eqs. (1) and (8) and ignoring the term $\frac{1}{2}$ for large p_g, we obtain

$$\gamma_g^2(0) = (nk)^2(\theta_c^2 - \theta\theta_c + \tfrac{1}{4}\theta_c^2\theta^2). \tag{16}$$

We neglect the term $\theta_c^2\theta^2$, which causes merely a correction of the order Δ^2 in the vicinity of $\theta = \theta_c$. The resulting curvature loss is

$$\alpha_g = 2nk(\theta_c^2 - \theta_c\theta)\exp\left[-\tfrac{2}{3}nkR\left(\theta_c^2 - \theta_c\theta - \frac{2a}{R}\right)^{3/2}\right]. \tag{17}$$

The exponential function in this expression agrees with that in the corresponding result of Ref. 8.

Figure 3 shows an evaluation of Eqs. (14) and (17) as a function of θ/θ_c for two guides 0.1 mm thick, one with a flat and one with a graded profile. We have used the parameters $n = 1.5$, $\Delta = 1\%$, $\lambda = 1\ \mu$m, and $R = 1$ cm. Note that the curvature loss (in dB/km) is plotted on a logarithmic scale. The losses in both guides increase sharply for angles θ close to the critical one. This increase is determined by a zero in the argument of the exponential functions in Eqs. (14) and (17). The angle at which the argument vanishes is

$$\theta_f = \theta_c(1 - 2a/R\theta_c^2)^{\frac{1}{2}} \tag{18}$$

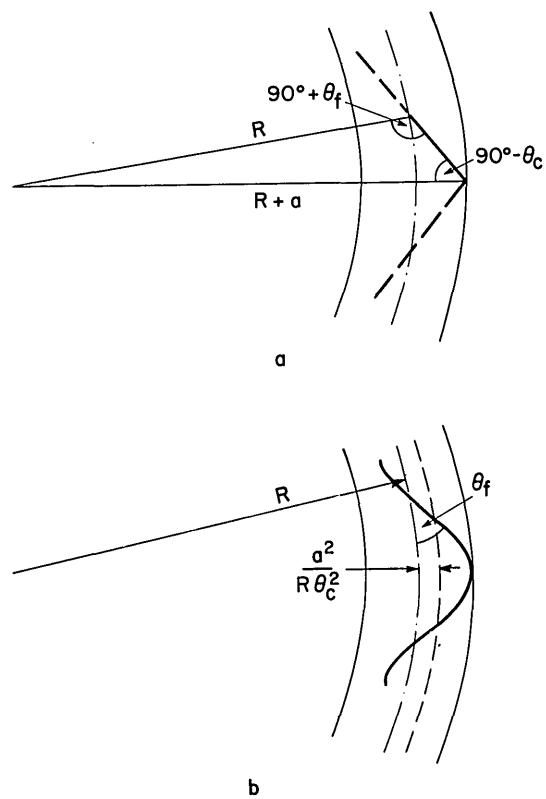

Fig. 4. Sketch of a curved dielectric guide showing the critical ray (a) for a flat and (b) for a graded core profile.

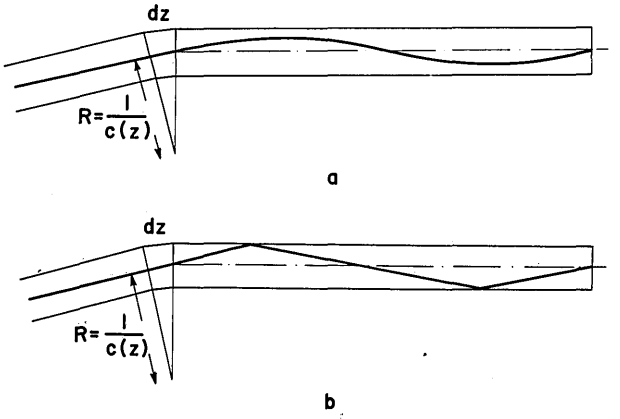

Fig. 5. Ray deflection in a curvature increment $c(z)dz$ (a) for a graded core and (b) for a homogeneous core.

for the flat guide and

$$\theta_g = \theta_c(1 - 2a/R\theta_c^2) \tag{19}$$

for the graded guide.

The curvature induced cutoff described by Eq. (18) can be explained in terms of ray optics. Figure 4(a) shows a curved guide and a ray being reflected at the critical angle at the outer interface. Using the triangle outlined in this sketch, we can calculate the angle θ_f at which this ray intersects the center line; we find

$$\cos\theta_f = (1 + a/R)\cos\theta_c. \tag{20}$$

By using the small-angle expansion of the cosine function we can transform this equation into

$$\theta_f = \theta_c(1 - 2a/R\theta_c^2)^{\frac{1}{2}}, \tag{21}$$

which agrees with Eq. (18).

Figure 4(b) shows a critical ray path in a curved graded guide. This path represents a sinusoidal oscillation about a center line which is displaced by $a^2/R\theta_c^2$ from the guide axis.[8,11] It is therefore given by the relation

$$r(z) = \frac{a^2}{R\theta_c^2} + \left(a - \frac{a^2}{R\theta_c^2}\right)\sin z\theta_c/a. \tag{22}$$

The angle at which this ray intersects the center of the guide is

$$\theta_f = \left.\frac{dr}{dz}\right|_{r=0} = \theta_c(1 - 2a/R\theta_c^2)^{\frac{1}{2}}, \tag{23}$$

which agrees with Eq. (21) but not with Eq. (19). The reason why the curvature correction $(1 - 2a/R\theta_c^2)^{\frac{1}{2}}$ enters the loss formula (19) with the second power is found in the fact that the bent graded guide reduces not only the possible ray angles but also their amplitudes. It is obvious from Fig. 4(b) that the inner part of the graded guide is not used in the bend. Since the total mode volume is proportional to the cone of available angles as well as the guide cross section, a curvature of the graded guide reduces its mode volume more severely than a bend in the homogeneous guide.

Although Eqs. (18) and (19) were derived for the two-dimensional model, at least Eq. (18) holds also for the cylindrical case.[16] Using Eqs. (1), (2), and (4) we can calculate the fraction of modes cost in a bent fiber:

$$y_f = (\theta_c^2 - \theta_f^2)/\theta_c^2 = a/R\Delta \tag{24}$$

and

$$y_g = (\theta_c^2 - \theta_g^2)/\theta_c^2 = 2a/R\Delta. \tag{25}$$

Higher powers of $a/R\Delta$ were neglected in Eq. (25). A comparison of Eqs. (24) and (25) shows that equal performance in gentle bends can be achieved, if the index difference in the graded profile is twice that of the flat profile. One-half of all modes (3 dB) are lost in the homogeneous fiber if the curvature radius equals the core diameter divided by the relative index difference. For $2a = 0.1$ mm and $\Delta = 0.01$ the radius is $R = 1$ cm.

IV. Ray Propagation in Randomly Curved Guides

After having gained some confidence in the ray representation and its applicability to curved multimode guides, let us utilize this formalism to investigate random bends. An excellent investigation of this kind was performed on parabolically graded cores by Unger.[11] He develops the ray equation for slowly changing curvatures

$$c(z) = 1/R(z) \tag{26}$$

and solves it for a ray that initially enters the guide on axis. He obtains for the ray position at the end of a guide of length L

$$r(L) = \frac{a}{\theta_c}\int_0^L \sin\left[\frac{\theta_c}{a}(L - z)\right] c(z)dz. \tag{27}$$

Differentiation of r with respect to L yields a similar equation for the ray angle:

$$\theta_g(L) = \int_0^L \cos\left[\frac{\theta_c}{a}(L - z)\right] c(z)dz. \tag{28}$$

An interpretation of Eq. (28) is given in Fig. 5(a). A guide segment dz with the curvature $c(z)$ deflects the ray by an angle $c(z)dr$ from its original path, which, in Fig. 5(a), was the guide axis. If there were no other curved segments present, the ray would pass the remaining guide length $L - z$ following a sine wave whose angle changes periodically as $c(z)dz\cos[\theta_c(L - z)/a]$. Equation (28) says that the effects of all curvature increments add linearly producing a compound deflection (or displacement) at the end of the guide.

Following the same argument we can easily establish a similar equation for the flat profile. In this case, a deflected ray follows a zigzag path as shown in Fig. 5(b). The angle at which it intersects the axis changes from θ to $-\theta$ twice every period $4a/\theta$. A curvature increment $c(z)dz$ at z produces therefore a deflection

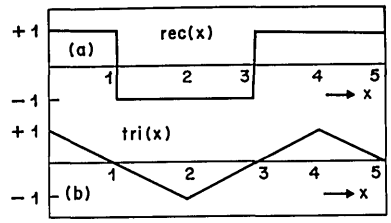

Fig. 6. Plot of the function rec(x) and tri(x) as used in the text.

$c(z)dz$ rec$[\theta(L - z)/a]$ at the end of the guide, where rec(x) is a binary function [see Fig. 6(a)] that changes from $+1$ to -1 at $x = 1,5,9,\ldots$ and from -1 to $+1$ at $x = 3,7,11\ldots$.

There is one important difference between the otherwise similar formalism of the graded and the flat profile. Contrary to the sinusoidal paths in a graded guide, which all have the same period $2\pi a/\theta_c$, the period $4a/\theta$ of a zigzag path in the flat profile depends on the angle θ of that specific path. If the angle changes—for example, as a result of a bend—the period changes with it. The wave optics equivalent of this ray period is the beat wavelength between consecutive modes. As a result of phase velocity differences, the mode fields lose and regain phase equality within a characteristic guide length, the beat wavelength, which coincides with the mean period of the two equivalent rays. Since, in the homogeneous guide, the phase velocity differences are mode dependent, the beat period changes with the mode number (and with the equivalent ray angle).

We must account for this change in period when we describe the deflection of a ray propagating in a guide with arbitrary curvature. Using the same argument that led to Eq. (28) we obtain for a ray that enters the guide at angle θ_0:

$$\theta(L)_0 = \theta_0 + \int_0^L \text{rec}[\theta(z)(L - z)/a]c(z)dz, \tag{29}$$

where $\theta(z)$ is the angle of the ray path at a point z along the guide. In a realistic guide, the influence of the curvature must be very small over a considerable guide length for the curvature loss to be tolerable. For most rays in a multimode guide, we can therefore replace $\theta(z)$ by θ_0 while integrating over a certain guide segment of length L. Very small input angles must of course be excluded from this approach; we shall consider them later.

For rays with some finite initial angle, the periodic reversal of the rec-function almost completely eliminates the effect of a long bend with constant curvature. This is obvious from Eq. (29). Even for the case of random curvature, Eq. (29) shows that the average ray deflection

$$\langle\theta(L)\rangle = \theta_0, \tag{30}$$

if the average is taken over an ensemble of statistically equivalent guides. It is the variance $\langle[\theta(L) - \theta_0]^2\rangle = \langle\theta^2(L)\rangle - \theta_0^2$ that yields a measure of the expected ray deflection.

We assume the curvature statistics to be such that the ensemble average $\langle c(z)c(z - u)\rangle$ is equal to the autocorrelation function $f(u)$ of curvatures spaced by a distance u along the same guide[11]; we assume also that f is independent of z, that is, the curvature statistics are the same everywhere along the guide. With

$$\langle c(z)c(z - u)\rangle = f(u), \tag{31}$$

and Eq. (29) squared and averaged over the ensemble, we obtain

$$\langle\theta^2(L)\rangle_f = \theta_0^2 + \int_0^L\int_0^L \text{rec}[\theta_0(L - z_1)/a] \times \text{rec}[\theta_0(L - z_2)/a]f(z_1 - z_2)dz_1dz_2. \tag{32}$$

The range of the double integration extends over the square area indicated by Fig. 7. The intersecting lines show zero crossings of the rec-functions. The rec-product of Eq. (32) is $+1$ in the white and -1 in the shaded areas. In reality, this checkerboard pattern is of course much finer, as there are hundreds of zero crossings within every meter of guide length.

To solve Eq. (32), we introduce a new coordinate system

$$v = \tfrac{1}{2}(z_1 + z_2) \tag{33}$$

and

$$u = z_1 - z_2,$$

which is also indicated in Fig. 7. We consider guide segments, whose length L is large compared to the distance over which the curvature is correlated. The autocorrelation function $f(u)$ then vanishes everywhere in Fig. 7 except for a narrow stripe along both sides of the main diagonal ($u = 0$). If we now integrate along u and v instead of z_1 and z_2, we may extend the integral over u from $-\infty$ to $+\infty$, since its value is limited by f and over v from 0 to L tolerating a small error in the lower left and the upper right corners of the square in Fig. 7. If we consider the fact that f is an even function of u, we have

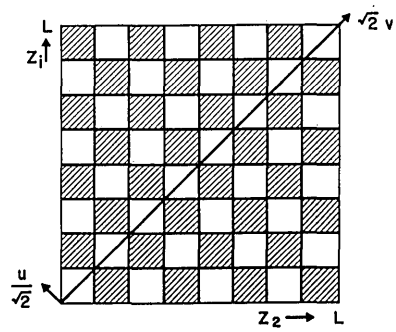

Fig. 7. Range of the double integration of Eq. (32). The rec-product in Eq. (32) is $+1$ in the white and -1 in the shaded areas. Also shown is the u, v-coordinate system used in Eq. (34).

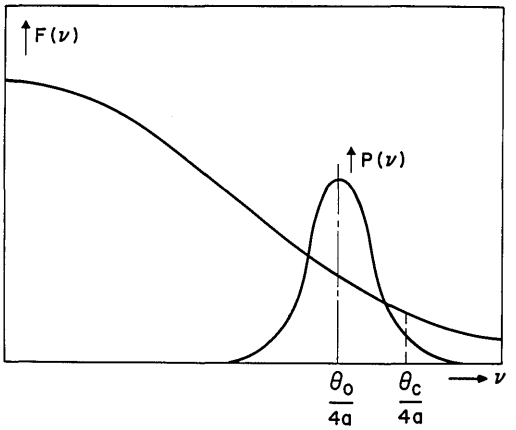

Fig. 8. Spectrum of possible guide curvatures and probability distribution of possible ray periods to be expected in a ray injected off-axis. The functional dependence is strictly speculative and merely meant for illustration.

$$\langle\theta^2\rangle_f = \theta_0^2 + 2\int_0^\infty f(u)du \int_0^L \mathrm{rec}\left[\theta_0\left(L - v - \frac{u}{2}\right)\Big/ a\right] \times \mathrm{rec}\left[\theta_0\left(L - v + \frac{u}{2}\right)\Big/ a\right]dv. \quad (34)$$

We can perform this integration after Fourier expansion of the rec-functions or just by inspection of the region of integration in Fig. 7. For the practical case that $L \gg a/\theta_0$, either approach leads to the result

$$\langle\theta^2\rangle_f = \theta_0^2 + L\int_0^\infty f(u)\,\mathrm{tri}(\theta_0 u/a)du, \quad (35)$$

where $\mathrm{tri}(x)$ is the triangular function shown in Fig. 6(b). This equation can be expressed in terms of the power spectrum

$$F(\nu) = \int_{-\infty}^{+\infty} f(u)\exp(i2\pi\nu u)du \quad (36)$$

of the curvature distribution. Expanding $\mathrm{tri}(x)$ in a Fourier series, we obtain

$$\langle\theta^2\rangle_f = \theta_0^2 + \frac{8L}{\pi^2}\sum_{m=0}^{\infty}\frac{(-1)^m}{(2m+1)^2}F\left[(2m+1)\frac{\theta_0}{4a}\right]. \quad (37)$$

According to Eq. (37), the rms increase in angle is determined by those components in the curvature spectrum whose frequency coincides with that of the zigzag ray or is a multiple of it.

The stiffness of practical fibers limits curvature components with mm-periods to very small amplitudes and practically excludes periods that are much smaller than that. Truncating Eq. (37) after the first term therefore yields a good approximation:

$$\langle\theta^2\rangle_f = \theta_0^2 + (8L/\pi^2)F(\theta_0/4a). \quad (38)$$

Since the next term of the series (37) is negative, the above approximation is conservative.

We have considered guide segments that are long compared to the zigzag period $4a/\theta_0$ and the curvature correlation distance but short enough so that curvature induced changes in the angle are small compared to θ_0. To shed some light on this latter requirement, Fig. 8 illustrates the spectral distribution of the curvature components. It also shows, for a guide segment of length L, the typical probability distribution of the expected ray frequencies. This distribution centers around $\theta_0/4a$ because of Eq. (30), while its variance increases proportional to L because of Eq. (38). The length L and the variance should be small enough that the statistical value $\theta(z)/4a$ can be replaced by the average value $\theta_0/4a$. This is a good approximation as long as $F(\nu)$ is well behaved and has no extrema in the range of significant ray probabilities.

In the case of a practical multimode fiber link, only a reasonably small fraction of the input power can be sacrificed in bends. This fraction will consist mostly of light entering the fiber close to the critical angle. Our principal interest is therefore in angles close to the critical one and in curvature distributions that increase this angle not too much. If the curvature distribution of such a guide has extrema around $\theta_c/4a$ this would indicate periodic deformations of a nonstatistical nature, which could and should be avoided. Excluding such artificial situations, we can justify using $F(\theta_0/4a)$ in Eq. (38) for the entire guide length. In the following estimate we go even a step further and replace $F(\theta_0/4a)$ by $F(\theta_c/4a)$.

This then permits an easy comparison with the parabolic profile for which[11]

$$\langle\theta^2\rangle_g = \theta_0^2 + (L/2)F(\theta_c/2\pi a). \quad (39)$$

The differences between Eqs. (38) and (39) are within the accuracy of these expressions and permit no conclusions as to the advantages of one or the other profile.

The results above were derived for the two-dimensional model, but the same arguments are applicable to the cylindrical case. Although this will result in somewhat different coefficients, the principal relations should be the same. For this reason, let us proceed in our estimate by simply applying Eqs. (38) and (39) to the cylindrical model. We calculate the input angle θ_0 whose rms increase leads to the critical angle. Because of Eqs. (2) and (4) the ratio $(\theta_c^2 - \theta_0^2)/\theta_c^2$ is the

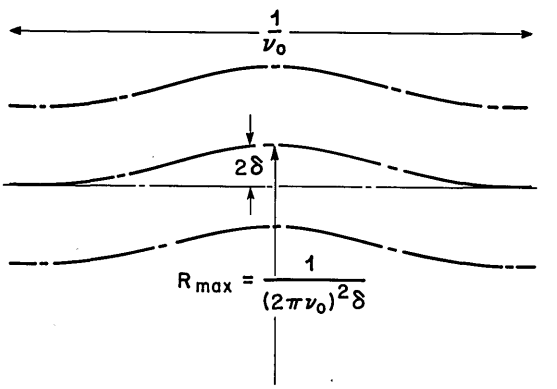

Fig. 9. Sinusoidal deviation from guide straightness used to interpret the curvature spectrum.

fraction of modes lost in random bends. Using Eqs. (1), (38), and (39) we obtain

$$y_f = (4L/\pi^2\Delta)F[(2\Delta)^{\frac{1}{2}}/4a] \tag{40}$$

and

$$y_g = (L/4\Delta)F[(2\Delta)^{\frac{1}{2}}/2\pi a]. \tag{41}$$

To gain an understanding of F at the critical ray frequency, let us consider a few specific examples. If the guide axis followed a sine wave of frequency ν_0 and amplitude δ, the curvature would be $(2\pi\nu_0)^2\delta \sin 2\pi\nu_0 z$. Let us assume that this sine-ripple extended only over a distance s and that the guide were otherwise straight. In this case, the curvature spectrum has a peak of height $(2\pi\nu_0)^4\delta^2 s^2/L$ and width $1/s$ at ν_0. Let us assume that there are η of these ripples (of length s) randomly distributed along a guide length L and with frequencies varying between $\nu_0 - 1/s$ and $\nu_0 + 1/s$. The various contributions to the curvature spectrum would then simply add and result in a value of approximately $\frac{1}{2}\eta(2\pi\nu_0)^4\delta^2 s^2/L$ at ν_0. Contributions from ripples outside the above frequency range would be negligible at ν_0.

Obviously, long natural ripples are very unlikely. For the sake of a simple example, let us assume that each ripple is just one period long. The ripple then degenerates to the single sinusoidal deviation illustrated in Fig. 9. With $s = 1/\nu_0$ we obtain

$$F(\nu_0) = 8\pi^4\nu_0^2\eta\delta^2/L. \tag{42}$$

After inserting this into Eqs. (40) and (41) we have

$$y_f = 4\pi^2\eta(\delta^2/a^2) \tag{43}$$

and

$$y_g = \pi^2\eta(\delta^2/a^2). \tag{44}$$

This result admits a simple physical interpretation, if one considers that Eqs. (43) and (44) represent the ratio $(\langle\theta^2\rangle - \theta_0^2)/\theta_c^2$. We can therefore rewrite Eqs. (43) and (44) in terms of the rms deviation of the angle θ:

$$(\langle\theta^2\rangle - \theta_0^2)_f^{\frac{1}{2}} = 2\pi(\delta/a)\theta_c(\eta)^{\frac{1}{2}} \tag{45}$$

for the flat profile and

$$(\langle\theta^2\rangle - \theta_0^2)_g^{\frac{1}{2}} = \pi(\delta/a)\theta_c(\eta)^{\frac{1}{2}} \tag{46}$$

for the graded profile. At least Eq. (46) is a straightforward result, which we could have obtained directly: A guide irregularity of the kind shown in Fig. 9 changes the ray angle in the graded profile[11] by $\pi\theta_c\delta/a$. Since the contributions add randomly the angle increases with $(\eta)^{\frac{1}{2}}$. The interesting result of our derivation is the fact that the length or period of such an irregularity can be quite different from the ray period and still contribute considerably to the rms increase of the angle. This follows from the wide spectrum that each individual irregularity covers in the curvature distribution.

We can now calculate the tolerable number or size of the irregularities. The quantity

$$\delta(\eta)^{\frac{1}{2}} = a/(8)^{\frac{1}{2}}\pi \tag{47}$$

produces a 3-dB mode loss in the homogeneous guide. If again $a = 50$ μm and $\Delta = 1\%$, $\delta(\eta)^{\frac{1}{2}} = 5.5$ μm. Thus, an irregularity of the kind illustrated in Fig. 9 with a deviation $2\delta = 0.5$ μm could be tolerated only about 500 times along the guide.

So far we have excluded the case of the on-axis or near-axis ray. We can study this problem at least formally, if we consider guide segments short compared to the total guide length L that produce only a small rms increase in the angle. We then write Eq. (38) in the form

$$\theta d\theta = (4/\pi^2)dLF(\theta/4a), \tag{48}$$

where now $F(\theta/4a)$ changes along the guide. By integrating Eq. (48) from the input angle θ_0 to the output angle θ_L, we obtain

$$\int_{\theta_0}^{\theta_L} \frac{\theta d\theta}{F(\theta/4a)} = \frac{4}{\pi^2} L. \tag{49}$$

To solve this equation, we must know the entire curvature distribution $F(\nu)$. If, for example,

$$F(\nu) = \langle c^2\rangle\, 2u_0/[1 + (2\pi\nu u_0)^2] \tag{50}$$

integration of Eq. (49) yields

$$L_f = \frac{\pi^2}{16}\frac{1}{u_0\langle c^2\rangle}(\theta_L^2 - \theta_0^2)\left[1 + \frac{\pi^2}{8}\frac{u_0^2}{a^2}(\theta_L^2 + \theta_0^2)\right]. \tag{51}$$

For the graded profile, inserting Eq. (50) into Eq. (39) results in a similar relation[11]:

$$L_g = (1/u_0\langle c^2\rangle)(\theta_L^2 - \theta_0^2)[1 + \theta_c^2(u_0^2/a^2)]. \tag{52}$$

If $\theta_0 = 0$ and $\theta_L = \theta_c$, Eqs. (51) and (52) determine the fiber length that an on-axis beam can travel before it is lost. With the realistic assumption that $u_0 \gg a/\theta_c$, we have approximately

$$L_f = 0.76\theta_c^4 u_0/\langle c^2\rangle a^2 \tag{53}$$

and

$$L_g = \theta_c^4 u_0/\langle c^2\rangle a^2, \tag{54}$$

where

$$\langle c^2\rangle = 2\int_0^\infty F(\nu)d\nu. \tag{55}$$

The quantity $\langle c^2\rangle^{-\frac{1}{2}}$ can be interpreted as the rms curvature radius and u_0 as the distance over which the curvature is correlated. For equal guide and curvature characteristics, an on-axis ray travels 1.3 times farther in the graded guide than in the homogeneous one. This comparison seems to indicate a disadvantage of the flat profile. The reason for this disadvantage is the poor guidance of near-axis rays that, because of their long zigzag period, interact with the larger (low-frequency) components of the curvature spectrum. We refrain from using Eqs. (53) and (54) in a numerical example, because we believe the assumption (50) to be so speculative that a quantitative evaluation could be very misleading.

VI. Conclusions

We have studied the performance of multimode fibers in bends and found a striking similarity between fibers with a graded core index (Selfoc) and a homogeneous core. The mode volume and the loss in bends are the same in both fibers, if the index difference of the graded profile (between core axis and cladding) is twice that of the flat profile. The critical radius of curvature (3-dB loss) is then equal to the core diameter divided by the (relative) index difference in the flat profile. This radius amounts to 1 cm for an index difference of 1% and a core diameter of 100 μm.

Mode coupling in random bends leads to a steady transfer of power from lower to higher modes and an eventual loss. Most critical are oscillating curvature components whose period coincides with the beat period between two modes (or the corresponding zigzag period of the equivalent ray). Even if these curvature components are very short—so short, in fact, that they degenerate to isolated hump-shaped deviations from straightness—they cause serious mode coupling. Five hundred of these irregularities, about 1 mm in length and 0.5 μm in size, result in a loss of half of the modes.

The author is grateful to E. A. J. Marcatili and D. Marcuse for fruitful discussions.

References

1. T. Uchida, M. Furukawa, I. Kitano, K. Kaizuki, and H. Matsumura, IEEE J. Quantum Electron. **QE-6,** 606 (1970).
2. E. G. Rawson, D. R. Herriott, and J. McKenna, Appl. Opt. **9,** 753 (1970).
3. S. Kawakami and T. Nishizawa, IEEE Trans. Microwave Theory Tech. **MTT-16,** 814 (1969).
4. D. Gloge, Proc. IEEE **58,** 1513 (1970).
5. E. A. J. Marcatili, Bell Syst. Tech. J. **48,** 2103 (1969).
6. E. A. J. Marcatili and S. E. Miller, Bell Syst. Tech. J. **48,** 2161 (1969).
7. V. V. Shevchenko, Izv. Vuz. Radiofiz. **14,** 768 (1971).
8. E. A. J. Marcatili, Bell Syst. Tech. J. **49,** 1645 (1970).
9. H. I. Heyke, H. Kirchhoff, and H. G. Unger, "Analysis of Optical Wave Launching and Propagation in Monomode and Multimode Fibers with Imperfections," Topical Meeting on Integrated Optics-Guided Waves, Materials, and Devices, 7–10 February 1972, Las Vegas, Nevada.
10. E. A. J. Marcatili, SPIE J. **8,** 101 (1970).
11. H. G. Unger, Arch. Elektrischen Uebertragung **19,** 189 (1964).
12. H. G. Unger, Arch. Elektrischen Uebertragung **24,** 101 (1970).
13. D. Marcuse, Bell Syst. Tech. J. **50,** 2551 (1971).
14. D. Gloge, Appl. Opt. **10,** 2252 (1971).
15. D. Gloge and D. Weiner, Bell Syst. Tech. J. **47,** 2095 (1966).
16. E. A. J. Marcatili, BTL; private communication.
